



**HAL**  
open science

# SMART-I<sup>2</sup>: A Spatial Multi-users Audio-visual Real Time Interactive Interface

Marc Rébillat, Etienne Corteel, Brian F.G. Katz

► **To cite this version:**

Marc Rébillat, Etienne Corteel, Brian F.G. Katz. SMART-I<sup>2</sup>: A Spatial Multi-users Audio-visual Real Time Interactive Interface. 125th Convention of the Audio Engineering Society, Oct 2008, San-Francisco, United States. pp.7609. hal-00619407

**HAL Id: hal-00619407**

**<https://hal.science/hal-00619407v1>**

Submitted on 6 Sep 2011

**HAL** is a multi-disciplinary open access archive for the deposit and dissemination of scientific research documents, whether they are published or not. The documents may come from teaching and research institutions in France or abroad, or from public or private research centers.

L'archive ouverte pluridisciplinaire **HAL**, est destinée au dépôt et à la diffusion de documents scientifiques de niveau recherche, publiés ou non, émanant des établissements d'enseignement et de recherche français ou étrangers, des laboratoires publics ou privés.

# SMART- $I^2$ : Spatial Multi-user Audio-Visual Real Time Interactive Interface

Marc Rébillat, marc.rebillat@limsi.fr  
Etienne Corteel, etienne.corteel@sonicemotion.com  
Brian F.G. Katz, brian.katz@limsi.fr

## Abstract

The SMART- $I^2$  aims at creating a precise and coherent virtual environment by providing users with both audio and visual accurate localization cues. It is known that for audio rendering, Wave Field Synthesis, and for visual rendering, Tracked Stereoscropy, individually permit high quality spatial immersion within an extended space. The proposed system combines these two rendering approaches through the use of a large Multi-Actuator Panel used as both a loudspeaker array and as a projection screen, considerably reducing audio-visual incoherencies. The system performance has been confirmed by an objective validation of the audio interface and a perceptual evaluation of the audio-visual rendering.

## 1 Introduction

In recent years, the advancement of immersive environments has separately produced systems with improved quality for 3D stereoscopic graphical rendering and also for 3D audio rendering. Despite these advances, few combined modality systems of high quality have been developed. This difficulty can be attributed to the different and stringent technical requirements for each rendering system, primarily in terms of equipment (construction material and placement). As so, these devices actually provide the users only a limited presence sensation.

In this paper, presence is understood as *"the perceptual illusion of non-mediation"* [1]. Many dimensions are involved in this high level cognitive process which includes communication and interaction. From a technological point of view, perceptual realism conveyed by the rendering interface is often thought of as a way to increase presence independently of the task or the content. The rendering device should not be detected by the user. It should be conceived as a large open window through which the users experience the virtual world. Users should have the impression of sharing the same space and should be able to interact together or within the environment. These aspects have lead to the conception of the SMART- $I^2$ .

In devices where a global audio rendering is chosen, rather than headphones (in CAVE-like environments for example [2][3], or frontal screen environments [4][5]), the optical pathways between the projector, screen, and the users eyes are often in conflict with the optimal acoustic pathways between loudspeakers and the users ears. So, some architectural and physical compromises must often be made in order to provide an effective audio-visual rendering, and loudspeakers are often placed behind or on the edges of the large rear-projection screen thereby reducing audio quality for the sake of graphical quality. The acoustical transmission characteristics of the screen and non-ideal positioning make it very difficult to achieve fine control of the acoustic field in the rendering zone. This is problematic for high quality precise advanced spatial rendering technologies such as Ambisonics [6], high order Ambisonics (HOA) [7], vector based amplitude panning (VBAP) [8] or wave field synthesis (WFS) [9]. Some solutions have been considered to compensate for the transmission characteristics effect of rear projection screens [10] but a fine acoustic control is still very difficult as loudspeaker placement is still highly guided by the optical pathways. Therefore, in such devices, perceptual realism is not

maximum.

Another common way to reproduce spatial audio is binaural rendering over headphones using the head-related transfer function (HRTF).[11] The quality of binaural rendering is highly linked to the use of an individual HRTF rather than a non-individual HRTF. In addition, head tracking and a dedicated rendering engine are usually necessary for each user. The use of headphones can reduce the level of immersion and also communication and interactivity for multi-user systems. Thus, loudspeaker reproduction has certain advantages over headphones, and is the option chosen in this system.

This research study presents a novel design concept, the SMART- $I^2$ , which attempts to resolve the problem of high quality immersive audio-visual rendering by rendering coherent audio and visual information. The sound rendering is realized using wave field synthesis technology (WFS) [9][12] which relies on physical based reproduction of sound fields within an extended listening area. The graphical scene is rendered using tracked stereoscopy [13], which presents users with the correct rendered visual image for each eye separately. Finally, these two technologies are combined together using two large Multi-Actuator Panels [14][15] which act both as projection screens and as loudspeaker arrays.

In this paper, the SMART- $I^2$  architecture is first described and technological choices are explained. The spatial audio-visual rendering of the SMART- $I^2$  is then assessed with a combined objective and subjective evaluation. The validation focuses on localization accuracy for both static and moving users.

## 2 The SMART- $I^2$ system

The SMART- $I^2$  system is an advanced audio-visual interface which results from the scientific collaboration of LIMSI-CNRS and sonic emotion. In this part, the key ideas of the system are explained and the realized system is later presented.

### 2.1 Audio-visual consistency over a large area

The key concept of the SMART- $I^2$  is to create a virtual window through which a plausible virtual world is perceived. All the spatial properties of the audio-visual scene should be accurately conveyed to the user(s) at any point within the rendering area. This includes angular and distance perception which should remain accurate throughout. The audio-visual window therefore ensures that static but also dynamic localization cues, such as the motion parallax effect, are preserved. The motion parallax effect occurs when users are moving about the rendering area. This effect is linked to the user's ability to ascertain the positions of audio-visual objects using the relative movements of these objects. For example, in the scene presented in figure 1, the user can ascertain the relative distance between objects 1 and 2 by comparing all the distance and angular information coming from these objects when moving from point A to point B.

WFS rendering, using horizontal loudspeaker arrays, is often regarded as an acoustical window which is limited by the array extension. For a linear array, the audio rendering is therefore limited to the horizontal plane but remains valid within a large listening area which can be determined using visibility criteria of the source through the loudspeaker array. Unlike other loudspeaker based spatial rendering techniques, WFS naturally gives access to the "audio" motion parallax effect.

3D visual rendering requires one to independently address each eye of the user. The rendering should also be adapted to the position and orientation of the user in order to render always the correct point of view and to preserve the visual scene organisation (objects sizes and angular positions). This technique is referred to as tracked visual stereoscopy. It combines visual crosstalk cancellation using light polarization ("passive" stereoscopy) or time multiplexing ("active" stereoscopy) with the adaptation of graphic rendering to the current position of the user. The user should wear special glasses for visual crosstalk cancellation. These are special polarized glasses (different polarization for each eye and each projector) for passive stereoscopy and shutter glasses synchronised with the video rendering for active stereoscopy.

Active stereoscopy is the most efficient crosstalk cancellation technique. However, it is expensive since it requires electronic synchronization of the projectors and the glasses. It is also known to induce

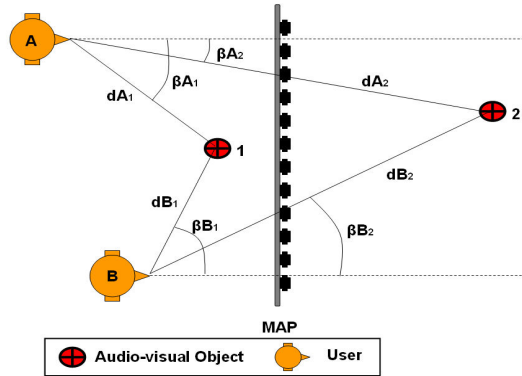


Figure 1: Illustration of the motion parallax effect.

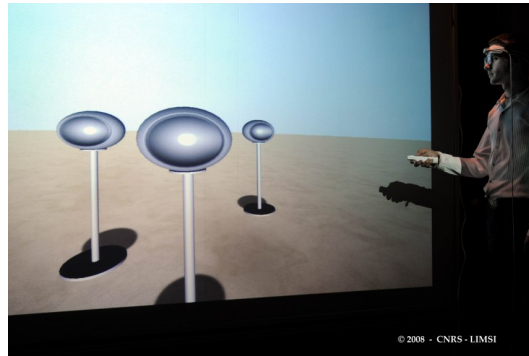


Figure 2: Overview of the SMART- $I^2$ .

visual fatigue which can be disturbing in the long run. Therefore, it was chosen to rely on “passive” stereoscopy. Both techniques could also be combined to increase the number of users. This is a topic for further research.

WFS and tracked stereoscopy can both be thought as a perceptual window opening onto a virtual world. They are thus coherent technological choices.

## 2.2 Overview of the system

The SMART- $I^2$  project was conceived as a large audio-visual window where the screens would also act as loudspeakers using WFS rendering. The installation of the system at LIMSI-CNRS is shown in figure 3. Two large screens form a corner so that the system presents a wide angular opening and a large listening area ( $2.5 \text{ m} \times 2.5 \text{ m}$ ). This corner installation poses less constraints, avoiding many of the common practical and acoustical concerns of a partly closed box as used in large CAVE systems. The walls and ceiling of the current installation are mostly covered with 2” acoustics foam to limit reflections. For the current validation study, only one screen is mounted (see figure 2).

## 2.3 Large MAP as a projection screen and loudspeakers array

MAP loudspeakers are derived from DML technologies. The panels are constructed of a light and stiff material on which multiple actuators are attached. Each actuator is independently driven. A multichannel loudspeaker is thus realized with a single unique physical structure.

Thanks to their low visual profile, multiple MAP loudspeakers can provide seamless integration of tens to hundreds of loudspeakers in an existing environment. Due to the excitation nature of the

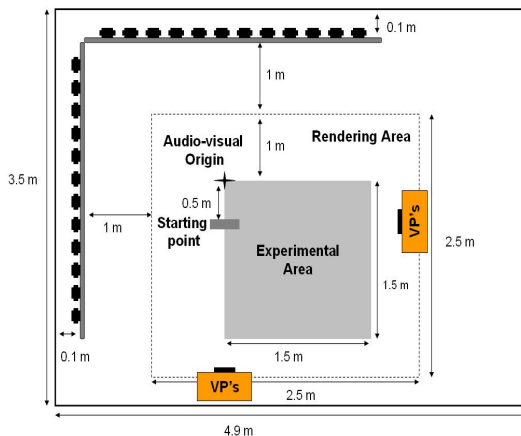


Figure 3: Schematic view of the SMART- $I^2$  installation.

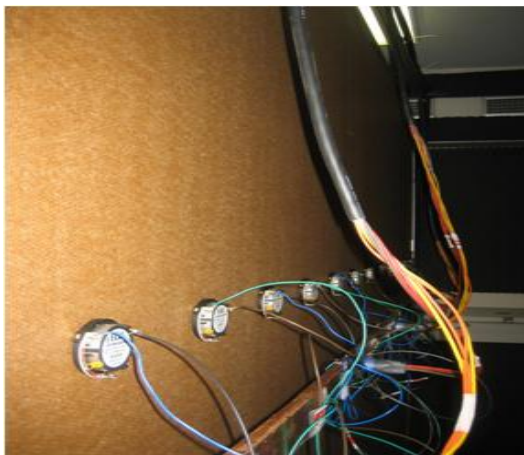


Figure 4: View of the back of the SMART- $I^2$  MAP.

panel, and their generally large size, displacement distances are very small and do not disturb 2D or even 3D video projection on the surface of the panel.

### 2.3.1 Design of the panels

The MAP used for the SMART- $I^2$  is a large honeycomb panel,  $2\text{ m} \times 2.66\text{ m}$ . The dimensions of the panel present a classical  $4/3$  ratio between height and width suitable for video projection. Twelve exciters are attached to the rear of the panel. They are located on a horizontal line every 20 cm. Such spacing corresponds to an aliasing frequency of about 1500 Hz accounting for the loudspeaker array size and the extension of the listening area.[17] This aliasing frequency assures an efficient spatial audio rendering. Some strategies are available to further raise the aliasing frequency.[18]

The front face of the panel has been treated with a metallic paint designed to maintain light polarization thus allowing for the use of passive stereoscopic projection. The panel is mounted in an aluminum frame such that the exciter array is at a height of 1.5 m (see figure 4). This positioning ensures that the horizontal plane where audio reproduction is correct corresponds to typical ear height for the majority of users.

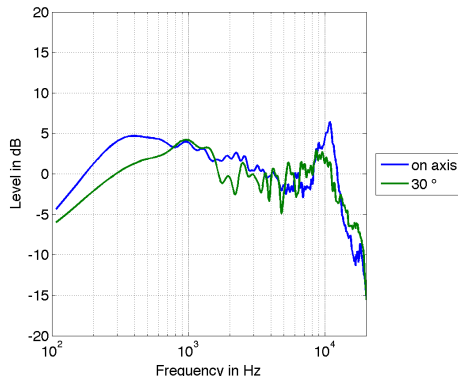


Figure 5: Frequency response of the large MAP used for SMART- $I^2$ .

### 2.3.2 Validity of the MAP for WFS

It has been shown that MAPs can be used for WFS rendering.[14][15] However, panels considered in previous studies were significantly smaller (40 cm  $\times$  60 cm or 133 cm  $\times$  67 cm) than those used here. Pueo *et al.* recently studied larger panels [16], showing measurements of reproduced sound fields using a 2.44 m wide and 1.44 m high panel. These objective results tend to confirm the potential use of such large panels for WFS, which should nevertheless be confirmed by further perceptual studies.

The typical frequency response of a MAP is not as optimized as electrodynamic loudspeakers, and a large MAP is not expected to have the same radiation as smaller scale MAP loudspeakers. In figure 5, the frequency response of the MAP designed for the SMART- $I^2$  is given for a central exciter, measured at 60 cm in front of the panel on-axis and at 30°. It can be seen the global frequency response is reasonably flat ( $\pm 5$  dB between 100 Hz and 15 kHz). The frequency responses measured on axis and at 30° off axis are similar. The level is somewhat reduced below 750 Hz by about 3 dB at 30° as compared to on-axis. A full study, including directivity patterns, is a topic for future research.

The frequency response of the large MAP seems appropriate for WFS rendering. In this study, only a naive equalization method is used which compensates for the global radiated response of the loudspeaker array (individual equalization, [12]). Advanced multichannel equalization techniques will be employed in further studies.

## 2.4 Rendering architecture of the system

The architecture of the SMART- $I^2$  is composed of three rendering components:

- *Virtual Choreographer (VirChor)*: An open source real-time 3D graphics engine that relies on an XML-based definition of 3D scenes with graphic and sonic components.[21][22]
- *The WFS Engine*: A real-time audio engine dedicated to low latency (less than 6 ms) WFS rendering which realizes the real-time filtering of up to 24 input channels (virtual sources) to 24 output channels (every exciter of the two MAPs).
- *Max/MSP*: A real-time audio analysis/synthesis engine using a graphical programming environment that provides user interface, timing, and communications.[23]

The audio visual scene description is based on the “Scene Modeler” architecture [24], which is a generic package for virtual audio-visual interactive real-time environment creation using both Max/MSP and VirChor. The Model-View-Controller organisation of the system [25] is depicted in figure 6.

For real-time rendering, two separated computers are used. On the main machine, Max/MSP and VirChor are running simultaneously. VirChor manages the virtual scene and graphical rendering. Max/MSP receives scene information from VirChor and is responsible for generating the audio content

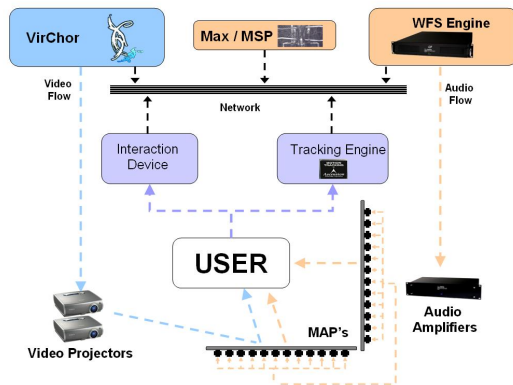


Figure 6: Model-View-Controller organisation of the SMART- $I^2$ .

of the scene. Audio channels are sent to the WFS engine which creates the driving signals for the exciters.

All rendering components are connected on a network which transmits the scene description (position of audio-visual objects, position/orientation of users provided by tracking devices, interaction parameters, basic services: start, stop rendering, shutdown machines...). This information is used to perform real-time updates of both the audio and graphic rendering, making the system fully interactive.

### 3 Evaluation of the SMART- $I^2$ spatial rendering

In this section, we focus on the evaluation of the spatial rendering quality of the SMART- $I^2$  interface. The evaluation combines an objective analysis of the binaural signals at the user’s ear and a subjective analysis based on listening tests.

#### 3.1 Presentation of objective analysis

The objective analysis presented here is similar to an earlier work by Sanson, Corteel and Warusfel.[19] Sanson *et al.* proposed a combined objective and subjective analysis of localization accuracy in WFS using individual HRTFs to binaurally render simulated virtual WFS configurations over headphones.

##### 3.1.1 Method

The method used here consists in estimating the localization accuracy of a given loudspeaker based spatial rendering technique using measured or simulated binaural impulse responses.

This method is composed of five steps illustrated in figure 7:

1. Binaural measurement of a dummy head in an anechoic chamber for a large number of positions (typically every  $5^\circ$  in both azimuth and elevation).
2. Binaural impulse responses on site measurement or estimation (from anechoic binaural measurements [19]) at given listening positions.
3. Estimation of “synthesized” binaural impulse responses for a given virtual source by summing the respective contribution of each array transducer.
4. Computation of localization cues (Interaural Time Differences (ITD) and Interaural Level Differences (ILD)) for both “ideal” and “synthesized” binaural impulse responses in auditory bands (40 ERB bands between 100 Hz and 20 kHz).<sup>1</sup>

<sup>1</sup>For a complete description of the ITD and the ILD extraction process, please refer to [19]

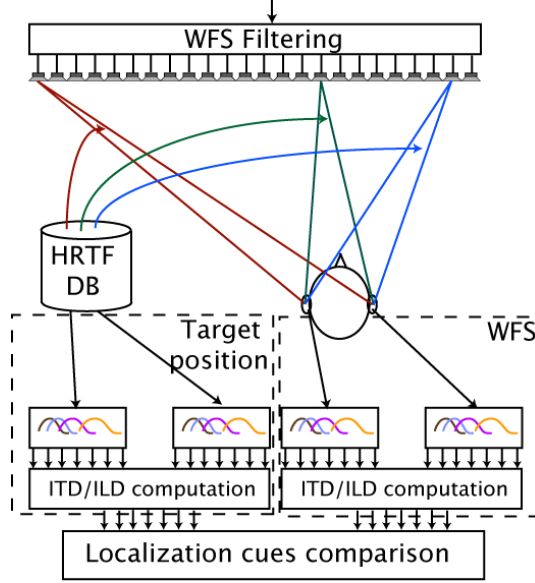


Figure 7: Extraction of objective localization cues.

5. Computation of ITD error,  $ITD_{err}(f_c(n))$ , and ILD error,  $ILD_{err}(f_c(n))$ , in each ERB frequency band where  $n$  ( $f_c(n)$ ) is the center frequency of the ERB band  $n$ .

The “ideal” impulse response is extracted from the database of anechoic impulse responses according to the virtual source and the listening position.

Global frequency independent localization accuracy criterion can finally be extracted using the weighting function  $q(f)$  proposed by Stern *et al.* in [20] that accounts for the relative importance of frequency bands to localization. Here a normalized weighting function,  $q_{norm}(f)$ , is defined as:

$$q_{norm}(f) = \frac{q(f)}{\text{mean}_{n=1..40}(q(f_c(n)))}. \quad (1)$$

The global ITD bias,  $B_{ITD}$ , is then defined as:

$$B_{ITD} = \text{mean}[ITD_{err}(f_c(n))q_{norm}(f_c(n))], \quad (2)$$

and the ITD variability,  $V_{ITD}$ , as:

$$V_{ITD} = \text{std}[ITD_{err}(f_c(n))q_{norm}(f_c(n))], \quad (3)$$

where *std* is the standard deviation. Similarly, an ILD bias,  $B_{ILD}$ , and ILD variability,  $V_{ILD}$ , are defined as:

$$B_{ILD} = \text{mean}[ILD_{err}(f_c(n))q_{norm}(f_c(n))], \quad (4)$$

and

$$V_{ILD} = \text{std}[ILD_{err}(f_c(n))q_{norm}(f_c(n))]. \quad (5)$$

These criteria are given here for wide band stimuli. In cases where the stimuli has only energy in a limited number of frequency bands, the criteria can easily be adapted to account only for these as proposed in [19].<sup>2</sup>

<sup>2</sup>The criteria presented here intend to provide a more consistent naming convention than that used in [19]. They are however very similar in their definition to the  $Mean_{err}$  and  $Std_{err}$  criteria defined for ITD and ILD in [19].



### 3.1.2 Interpretation of the objective localization criteria

The bias measures  $B_{ITD}$  and  $B_{ILD}$  indicate the average offset of the conveyed ITD and ILD respectively, compared to the reference (anechoic) ITD and ILD respectively, at the target position. It might be interpreted as an indication of a potential perceptual shift in azimuth due to distorted localization cues conveyed by the considered reproduction setup. The suggested shift would be to the right for positive values or to the left for negative values. The variability measures  $V_{ITD}$  and  $V_{ILD}$  are an indication of the consistency of the localization cues among the frequency bands. It might thus be considered as an indication of the locatedness of the synthesized virtual source.

In [19], Sanson *et al.* show that the absolute localization bias for WFS does not typically exceed  $5^\circ$  independently of the loudspeaker spacing (15 cm or 30 cm in this study) considering large band stimuli covering the entire audible frequency range (white noise) and virtual sources located behind the loudspeaker array. The absolute localization bias typically increased from  $7^\circ$  to  $10^\circ$  for high-passed noises with cutoff frequencies of 750 Hz, 1500 Hz, and 3000 Hz. The associated analysis showed that, in some cases, the ITD and ILD errors were indicating conflicting directions which could be attributed to the finite length of the loudspeaker array. Then, in most of these cases, the ILD cues were dominating which may be due to the frequency content of the employed stimuli (high-passed white noise) and possibly the large variability of the ITD (typically above 0.3 ms). Only in cases where the ILD error is low (typically below 1 dB), the ITD was the dominant cue ( $4^\circ$  localization bias for a target at  $+25^\circ$ ,  $B_{ITD} = 0.05$  ms and  $V_{ITD} = 0.15$  ms).

It should be clear, however, that the objective criteria presented here are meant as comparison indicators to provide hints about the differences observed between situations. The localization model is rather naive and does not pretend to provide an absolute predictor of localization.

## 3.2 Presentation of the evaluation

A joint subjective/objective evaluation of the spatial audio rendering of the SMART- $I^2$  was conducted to evaluate its consistency with 3D graphics rendering.

Two perceptual experiments were carried out:

1. A traditional azimuth localization task where stationary subjects have to identify which of a series of visual object positioned on an arc corresponds to the position of a hear sound source.
2. A spatial exploration task which focuses on the evaluation of the parallax effect rendering in which a series of visual object are positioned on a line perpendicular to the screen and subjects are instructed to wander about the experimental area to identify which of them is the source of the sound.

In parallel to these experiments, individual exciters of the SMART- $I^2$  were measured in the experimental area using a dummy head (Neumann KU-100). Figure 8 presents a top view the position of the virtual sources for each experiment and the positions at which the dummy head was located. The dummy head was positioned at 36 different locations on a regular grid, grid spacing of 30 cm in both  $X$  and  $Y$ , so as to cover the entire experimental area in which subjects could move during the experiments.

Bias and variability criteria are computed for all measured listening positions and virtual sources used in the subjective experiments. The artificial head was always facing the screen, orientated towards the  $Y$  axis of figure 8.

These criteria are also computed for a virtual WFS setup composed of 12 ideal omnidirectional loudspeakers in an anechoic environment. This simulates an “ideal” WFS setup using loudspeakers at the same position as the exciters in the SMART- $I^2$  based on previous anechoic measurements of the dummy head. As such, our results can be compared with those of Sanson *et al.* [19] and any observed inaccuracies could be attributed either to known WFS deficiencies (diffraction, aliasing) or to the specific radiation characteristics of the large MAP.

The subjective experiment is organised in 3 parts performed during one 40 minute session:

1. The test scene.

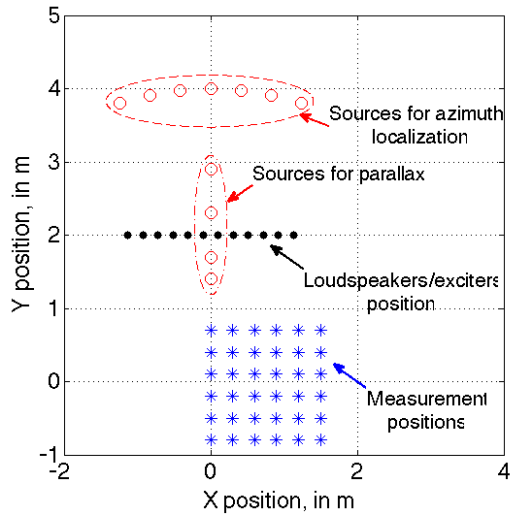


Figure 8: Top view of the installation, position of screen, audio target sources for subjective experiments and measurement points spanning the test experimental area.

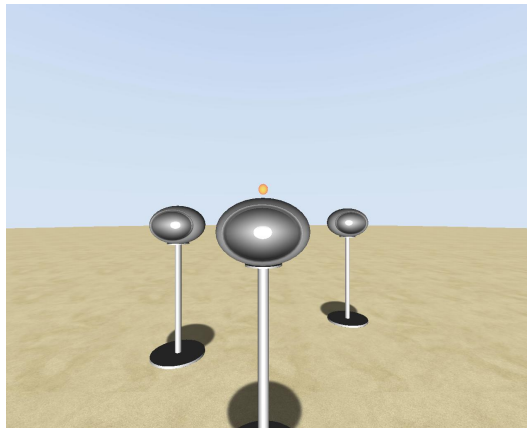


Figure 9: Introductory scene.

2. The azimuth localization task.
3. The parallax effect validation task.

Fourteen subjects (9 male and 5 female) ranging from 22 to 53 years old participated in the experiment. No subject was visually or auditory impaired. For half of the subjects, the parallax effect validation task was performed before the azimuth localization task in order to evaluate the influence of learning or habituation on the results of either task. Analysis confirmed that there was no significant effect on the results due to task order. The introductory scene contained three virtual visual loudspeakers placed on a neutral background (see figure 9). Only one, indicated by the orange cursor above, is activate and plays music. The subject can choose which loudspeaker is active using a Wiimote. The subject is also free to move within the rendering area to get accustomed to tracked stereoscopy and WFS. During this introductory scene, the stereoscopic rendering parameters were adjusted to the individual subject.

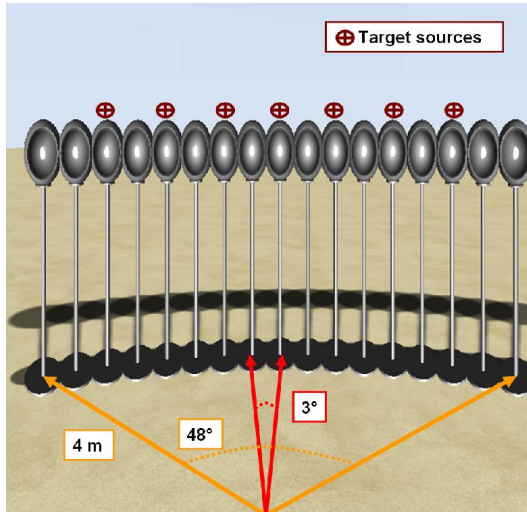


Figure 10: The audio-visual scene for azimuth localization accuracy. The 7 potential acoustic target positions are indicated here.

## 4 Azimuth Localization Evaluation

### 4.1 Experimental Protocol

The goal of this experiment is to evaluate the localization accuracy of the spatial audio rendering of the SMART- $I^2$ . The audio-visual scene contains 17 virtual visual loudspeakers distributed on an arc and at 4 m from the audio-visual origin (see figure 10). Virtual loudspeakers are separated by  $3^\circ$  which provides a  $48^\circ$  angular aperture.

The position of the visual objects has been chosen to be smaller or equal to the human audio azimuth resolution (i.e.  $3\text{-}4^\circ$ , see [26]). Moreover, all visual objects are similar. This creates multiple visual distractors that limit bias due to audio-visual integration, the so-called ventriloquism effect [27].

A single white noise burst of 150 ms with 10 ms onset and offset (Hanning window) was presented at nominal level of 68 dBA from one of the 7 target sources, indicated in figure 10 (background noise level at subject position was 40 dBA). The subject’s task was to indicate from which of the 17 visual objects the sound has been emitted. The subject had no prior knowledge of possible target locations.

At the beginning of the experiment, the subject was positioned at the starting point (see 3), and instructed to remain there. There were 15 repetitions of the 7 potential positions corresponding to a total number of 105 trials. At the beginning of each trial, a position is randomly picked. Each trial is organized in the following way:

1. The subject indicates that he is ready by pressing a button.
2. His position and head orientation are checked with the tracking engine.
3. If the subject is ready and his head orientation is correct, the sound stimulus is played once.
4. A visual selector appears (cf. figure 11), and the subject indicates the perceived location of the sound source by moving the cursor on top of the corresponding visual object.

### 4.2 Results of the subjective evaluation

Each trial was performed in a mean time of  $5.8 \pm 3.8$  sec. Angles are given clockwise. A Lilliefors test rejected the null hypothesis that the empirical distribution (result values) follows a normal

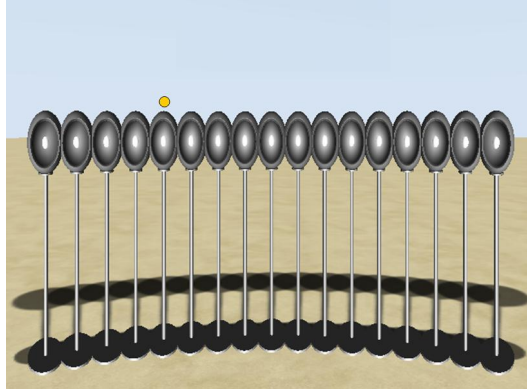


Figure 11: The scene as viewed by the user (step 3).

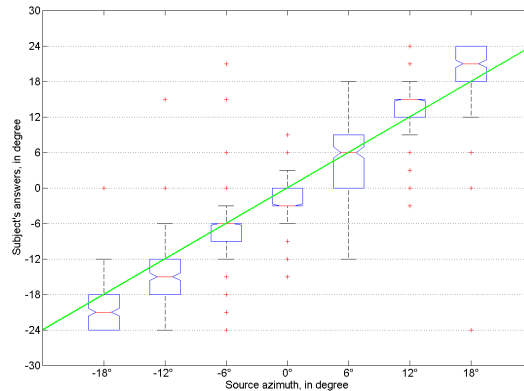


Figure 12: Subjects answers for the target sources.

distribution. The Lilliefors test is a Kolmogorov-Smirnov type test where the empirical distribution function is compared to a normal distribution with the mean and standard deviation equal to the empirical ones. Therefore, it was decided to use a quantile repartition for the analysis of the results which is presented in figure 12. The displayed boxes have lines at the lower quartile, median, and upper quartile values. As a measure of variability, we chose the half inter-quartile range ( $HIQR = (P(75\%) - P(25\%))/2$ ) where  $P(X)$  is the percentile function which gives the value in the data set under which are found  $X\%$  of the values. The half inter-quartile range is presented since its interpretation is close to the standard deviation used in literature in order to facilitate comparisons with previous localization studies. The whiskers displayed in figure 12 (lines extending from each end of the boxes) show the extreme values beyond the lower and the upper quartiles. Outliers are data with values beyond the ends of the whiskers and are indicated with a red '+'. The notches represent an estimate of the uncertainty about the medians. The different target sources can thus be considered to be well identified by subjects in this task since notches are non-overlapping in figure 12.

The median of the error is always smaller or equal to  $3^\circ$ , which is the angular separation between two neighbouring speakers. For extremal target sources on the left the median error is close to  $-3^\circ$ , and for the ones on the right to  $3^\circ$ . This denotes a tendency to exaggerate the angular position of lateral sources. The  $HIQR$  is always lower than  $3^\circ$ , except for the source placed at  $6^\circ$  for which it reaches  $4^\circ$ .

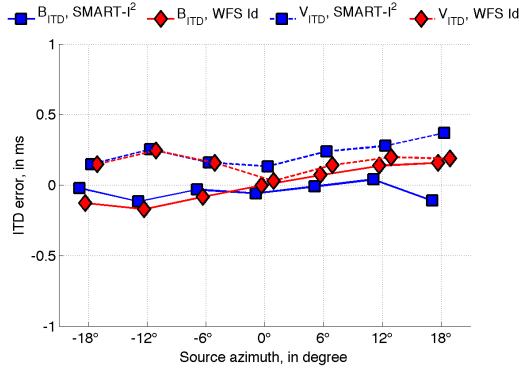


Figure 13:  $B_{ITD}$  and  $V_{ITD}$  for SMART- $I^2$  and ideal loudspeakers ( $WFSId$ ), center position.

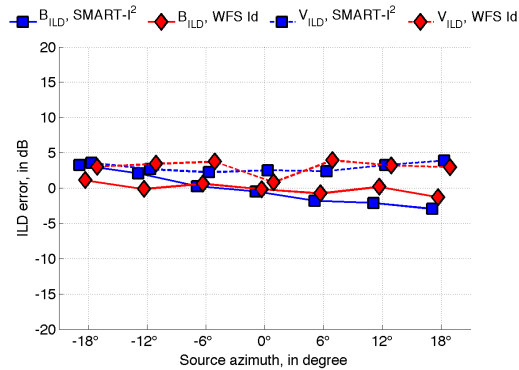


Figure 14:  $B_{ILD}$  and  $V_{ILD}$  for SMART- $I^2$  and ideal loudspeakers ( $WFSId$ ), center position.

### 4.3 Results of the objective evaluation

The bias and variability for ITD and ILD are displayed in figures 13 and 14 at the position of the subjects for all sources used in the localization test.

The errors for localization cues remain relatively small for the SMART- $I^2$  and are comparable to errors obtained with the ideal WFS setup. However, the variability of the ITD is slightly higher for the SMART- $I^2$  than for the ideal WFS setup. The ILD bias exhibits a curve which would suggest a compression of the perceived azimuth of virtual sources. This is an opposite effect that was noticed in the subjective test indicating a moderate dilatation of the perceived azimuth.

### 4.4 Discussion

The azimuth localization task was reported by the users to be quite easy and intuitive. In this section, the results are discussed and compared with similar previous studies. The validity of localization in the complete listening area is verified further on.

#### 4.4.1 Comparison with other studies

The absolute human localization blur, according to [26], is between  $1^\circ$  and  $4^\circ$  in front of the listener, depending on the test signal and on the reporting method. The absolute localization bias of the present study is thus very close to human ability.

The observed extra-lateralization has no precise explanation. It should be recalled that the localization model used in the objective part of this study is rather naive. It does not account for the precedence effect. The angular localization is indeed biased in our environment. This could be due to residual reflections from the side wall which cannot be properly taken into account in the model, but this rationale does not fully explain the results. Interestingly, this effect has also been reported to the same extent ( $2^\circ$  to  $3^\circ$  over-lateralization at  $\pm 20^\circ$  or  $30^\circ$ ) in headphone-based localization experiments using individual HRTFs [32][33]. As such, one cannot claim this as a system default, but could be more linked to some perceptual criteria.

Verheijen achieved localization experiments on a WFS setup composed of 24 loudspeakers with an 11 cm spacing using a similar method where the subjects had to indicate which of the visible (real) loudspeakers was emitting sound for both synthesised sources, using WFS, and real sources.[29] Verheijen also tested a loudspeaker spacing of 22 cm using thus only 12 loudspeakers as in the current study. Verheijen reported mean localization error for synthesized sources of approximately  $3.5^\circ$  independent of loudspeaker spacing. The associated standard deviation was  $1.5^\circ$ . Localization accuracy for real sources was very similar.

The localization accuracy provided by the SMART- $I^2$  is comparable to these results for a similar WFS configuration. However, the *HIQR* obtained with the SMART- $I^2$  is higher than the standard deviation shown there. This may be attributed to the radiation characteristics of the MAP loudspeakers as compared to those of electrodynamic loudspeakers as used by Verheijen. It is expected that the use of advanced multichannel equalization techniques [12] will increase the localization accuracy in SMART- $I^2$ . This will be a topic for further studies.

The SMART- $I^2$  results should also be compared to results provided by other sound rendering technologies. For an ideal fourth order ambisonic rendering, with a circular 12 loudspeaker array, Bertet *et al.* reported a median error is between  $1^\circ$  and  $3^\circ$  and a *HIQR* between  $2^\circ$  and  $5^\circ$  at the sweet spot.[30] According to [31], a binaural rendering using individual HRTFs showed an average absolute localization error of  $0^\circ$  to  $3.5^\circ$  depending on source azimuth (from  $-30^\circ$  to  $+30^\circ$  every  $10^\circ$ ) with a standard deviation of  $6^\circ$  to  $9^\circ$ . The latter study also included a combined audio-visual study which showed that audio-visual integration occurs and that there is a dominance of visual localization over auditory localization which removes the bias and reduced the standard deviation to  $2.1^\circ$  in bimodal conditions. A similar effect can be expected in the SMART- $I^2$  system for congruent audio-visual objects.

#### 4.4.2 Extension to entire listening area

Figures 15 and 16 present ITD and ILD bias (solid line) and variability (dashed line) criteria averaged over all measured positions (cf. figure 8). Whiskers indicate standard deviation.

Averaged ITD and ILD bias and variability criteria follow similar tendencies as those observed for the center position. Moreover, the standard deviation of these criteria remains low, typically below 0.1 ms for ITD based criteria and below 1 dB for ILD based criteria. It can thus be expected that localization remains almost unbiased over the entire listening area with a reduced localization accuracy for side virtual sources as in the center listening position. Localization accuracy can thus be expected to be at least as good as sweet spot based techniques such as fourth order ambisonics but over an extended listening area.

## 5 Parallax effect evaluation

### 5.1 Experimental protocol

The audio-visual scene contains 8 “visual” loudspeakers arranged in a line perpendicular to the screen at 30 cm intervals. The first loudspeaker is 1.1 m away from the audio-visual origin (see figure 17), resulting in the three first loudspeakers being in front of the screen. Only 4 of the visual target sources are used as audio targets in this session (1.4 m, 1.7 m, 2.3 m and 2.9 m). The audio stimulus is a 1 sec white noise burst, low pass filtered at 4 kHz, on which a 18 Hz amplitude modulation is applied (70 dBA presentation level at the audio-visual origin) followed by a 1 sec silence. The stimulus was

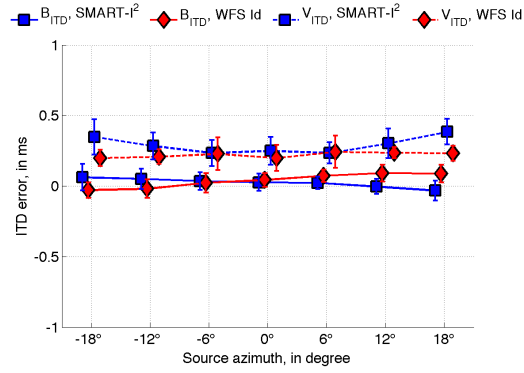


Figure 15:  $B_{ITD}$  and  $V_{ITD}$  for SMART- $I^2$  and ideal loudspeakers ( $WFSId$ ), average over all measured positions.

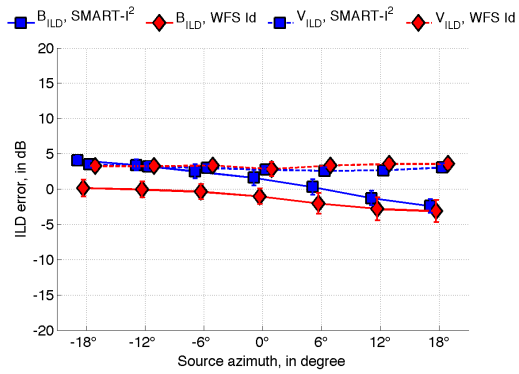


Figure 16:  $B_{ILD}$  and  $V_{ILD}$  for SMART- $I^2$  and ideal loudspeakers ( $WFSId$ ), average over all measured positions.

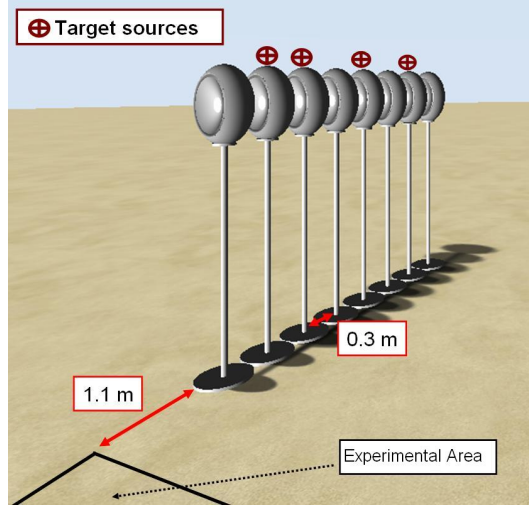


Figure 17: The audio-visual scene for parallax effect evaluation in the SMART- $I^2$ .

played continuously until the subjects made their selection. The sound levels of the different sources were chosen in order to have the same effective level at the audio-visual origin. Parallax was thus the only available cue to the subjects for distance estimation. There were 10 repetitions of each of the 4 target positions corresponding to a total number of 40 trials. In this experiment, subjects were instructed to move about within the defined experimental area (see figure 3). Each trial begins with the user located at the starting point. Subjects are instructed to move slowly from this point to the right of the listening area. The experimental procedure was the same as previously described. Subject position was checked before the beginning of the trial but not the head orientation.

## 5.2 Results of the subjective evaluation

The results for parallax evaluation are presented in figures 18 and 19 in the same manner than the previous results. The average response time for each trial is  $23 \pm 13$  sec with little variation between source positions. In figure 18, the different data sets corresponding to the target sources are not clearly separated. The second source (1.7 m: focused source) is perceived to be at the relative position of the third source (2.3 m: source behind the screen). The two other sources are well identified. The *HIQR* in meters can be seen in figure 18. It is minimum for the closest source (1.4 m) where it reaches 0.15 m. The *HIQR* is 0.45 m for the source at 1.7 m, and approximately 0.3 m for the two others.

Figure 19 presents the median error and the *HIQR* converted into degrees as perceived at the extreme right listening position ( $x = 1.5$  m,  $y = 0$  m) which is the end of the path proposed in the instructions. This is the position in the experimental area (cf. figure 3) at which there is the maximum angular difference between visual objects. Therefore, this is the position where the subjects could most easily perform the required task.

Figure 19 shows that the median error is positive for the two first focused sources, null for the third one, and negative for the last one. This indicated that the two closest sources are biased to the right (further distance), the third source (at 2.3 m) is accurately localized whereas the last one is perceived too much to the left (closer to the screen location). The *HIQR* is close to  $4^\circ$  for all sources which is similar to the results of the first experiment. The estimation of degrees at this position provides an explanation for the large variation of *HIQR* observed in figure 18.



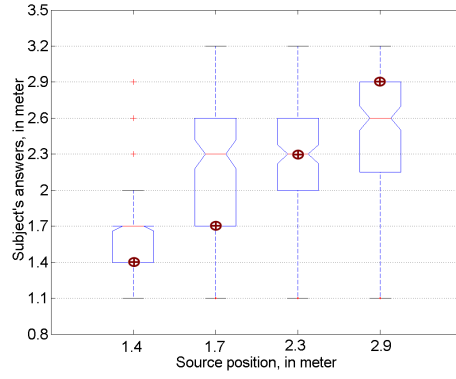


Figure 18: Subject responses for the target source distance position. Target locations are also indicated.

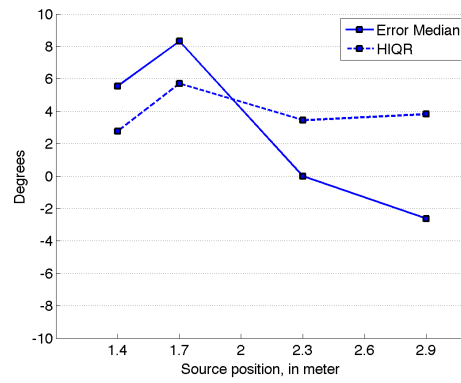


Figure 19: Median error and *HIQR* for the target sources. Errors are indicated in degrees as perceived at the extreme right listening position ( $x = 1.5$  m,  $y = 0$  m).

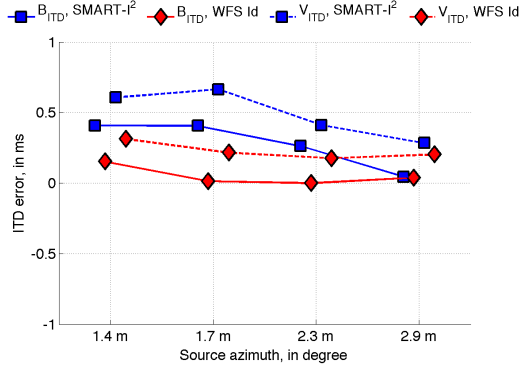


Figure 20:  $B_{ITD}$  and  $V_{ITD}$  for SMART- $I^2$  and ideal loudspeakers ( $WFSId$ ), extreme right listening position.

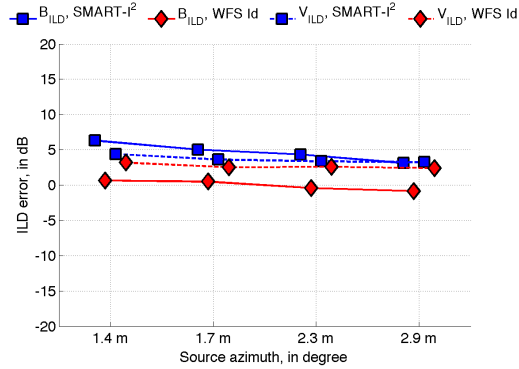


Figure 21:  $B_{ILD}$  and  $V_{ILD}$  for SMART- $I^2$  and ideal loudspeakers ( $WFSId$ ), extreme right listening position.

### 5.3 Results of the objective evaluation

During the experiment, subjects were instructed to follow the path between the center listening and an extreme side listening position ( $x = 1.5$  m,  $y = 0$  m in figure 8). At the center listening position, the ITD and ILD bias and variability are almost independent on the source distance and are therefore not presented here. At this position, ITD and ILD bias are in the range of  $0 \pm 0.05$  ms for both ideal WFS and SMART- $I^2$ ,  $0 \pm 0.5$  dB for ideal WFS and  $-1.5 \pm 0.5$  dB for SMART- $I^2$ . The small observed ILD bias for SMART- $I^2$  might be due to the presence of the wall in the current installation.

Objective criterion at the extreme right position ( $x = 1.5$  m,  $y = -0.5$  m in figure 8) are presented in figures 20 and 21. It can be seen that there is a positive bias ( $B_{ITD} \simeq 0.2$  ms and  $B_{ILD} \simeq 7$  dB) for sources located in front of the screen (distance lower than 2 m) synthesized using SMART- $I^2$ . This bias is not observed for ideal WFS. The consistent bias for both ITD and ILD might explain the overestimation of perceived distance in the subjective experiment. This might cause a localization bias to the right of the perceived azimuth of the source compared to the target azimuth.

For sources located behind the array, a positive bias is observed for  $ILD$  ( $B_{ILD} \simeq 5$  dB) whereas  $B_{ITD}$  is close to null. This may explain the limited bias in localization accuracy observed for these sources accounting for the dominance of ITD for large band stimuli [28].

## 5.4 Discussion

The subjects reported this task very difficult to perform. The subjects were all a bit disturbed by the missing “static” acoustical cues for distance perception (level differences, room effect, ...). During the first trials, subjects strategies were to explore the entire rendering area trying to find the best localization place. After that, 80% of the subjects went directly to the extreme right listening position to choose the loudspeaker, and the other part still proceed to a systematic exploration or to a random walking among the rendering area.

The motion parralax is a dynamic distance cue which is known to be not as salient as static distance cues.[34][35] In [34], blind-folded subjects were instructed to locate a sound source in a very similar way than our experiment. A number of loudspeakers were located on a line passing through the starting position at 2 m to 6 m from the starting position. The subjects were asked to walk either 2 m or 4 m in a direction perpendicular to this line while one loudspeakers was active (synthesized voice). The subjects were then instructed to report the exact location of the active source by walking to it. The results indicate an over-estimation of the distance of the closer sources and an under-estimation of the distant ones. The same phenomenom has been noticed in [35]. The standard deviation found in [34] was approximately 0.6 m, greater than the *HIQR* of our experiment. However, the reporting method we used is quite different than in [34] and [35]. The current study task can almost be considered as a localization task with visual cues seen from multiple listening positions.

The objective analysis revealed inconsistent localization cues which explain the localization bias for sources in front of the screen. In further studies, these errors should be compensated for using more advanced equalization techniques or by modifying the acoustical characteristics of the panel. Considering the furthest position (2.9 m), the compression in distance might also be due to the “natural” room effect of the real environment. The latter provides distance cues related to direct over reverberant energy which may bias distance perception towards the location of the screen.

From a visual point of view, a compression of distance perception has been noticed for a while in immersive virtual environments. It does not seem to be linked to the field of view and binocular viewing, and for the moment no convincing explanations has been found to this phenomenom.[36] In the SMART- $I^2$ , this can contribute to the mislocalization of the audio-visual objects in terms of distance.

In conclusion, it can be stated that the SMART- $I^2$ 's ability to render the audio-visual motion parralax effect is similar to the one observed with real sources. Therefore, it can be expected that the results would be improved using consistent level differences and virtual room effect. Audio-visual integration should also improve the precision of the motion parallax effect rendering in a similar way than for the localization accuracy for static users (cf discussion in section 4.4.1).

## 6 General discussion and conclusion

In this paper, an immersive audio-visual environment, the SMART- $I^2$ , has been presented and evaluated. The design focus was placed upon audio-visual consistency which may contribute to an increased feeling of presence in the virtual environment.

Subjects were globally satisfied with the proposed rendering. Further studies should be made with this system with more realistic audio-visual scenes to evaluate more precisely the perceptual realism provided by the SMART- $I^2$ . A more complete acoustical study of the large MAP is also required in order to increase the precision of the WFS rendering, especially for sources located in front of the screen.

The immersion quality was reported by the subjects to be sufficient and that they really felt they were “in the scene”. One fact that has been reported was that the limited size of the audio-visual window caused some disturbances in extremal positions. Installation of the second MAP will offer users a larger field of view and thus should raise up the immersion quality.

In these experiments, the level of interaction was very limited in terms of direct interaction with the scene and also interactions between multiple users. The addition of both may contribute to an increase in the sense of presence. This will be verified in further studies.

The global feeling about the audio-visual rendering provided by the SMART- $I^2$  was that the consistency between audio and visual features is very accurate and that immersion quality is already convincing. The SMART- $I^2$  was perceived as an audio-visual window opening into a plausible and consistent virtual world. The results of the objective analysis and subjective evaluation confirm that point. The localisation accuracy shown by subjects permits a global validation of the WFS rendering, the visual rendering and the audio-visual calibration.

## 7 Acknowledgements

This work was supported by CNRS and sonic emotion. The authors would like to thank Matthieu Courgeon, Rami Ajaj, Jonathan Chaboissier, Christian Jacquemin and Tifanie Bouchara for their support on the graphical part.

## References

- [1] Lombard M. and Ditton T., “At the heart of it all: The concept of presence”, *Journal of Computer-Mediated Communication*, **3**(2), September 1997.
- [2] Cruz-Neira C., Sandin D., DeFanti T., Kenyon R., Hart J., “The CAVE-Audio visual experience automatic virtual environment”, *Communications of ACM*, **35**(6), 64-72, 1992
- [3] EVE project homepage (Experimental Virtual Environment) <http://eve.hut.fi/>
- [4] de Bruijn W., “Application of Wave Field Synthesis for life-size videoconferencing” *Phd thesis*, Delft University of Technology, 2004.
- [5] Springer J.P., Sladeczek C., Scheffler M., Hochstrate J., Melchior F., Frohlich B., “Combining Wave Field Synthesis and Multi-Viewer Stereo Displays”, *Proceedings of the IEEE conference on Virtual Reality*, Washington, IEEE Computer Society, pp. 237-240, 2006.
- [6] Gerzon M. A., “Periphony: With-Height Sound Reproduction”, *Journal of the Audio Engineering Society*, **21**(1), pp. 2-10, 1973.
- [7] Daniel J., “Représentation de champs acoustiques, application à la reproduction et à la transmission de scènes sonores complexes dans un contexte multimédia”, *Ph.D. thesis*, University of Paris 6, Paris, France, 2000.
- [8] Pulkki V., “Virtual sound source positioning using vector base amplitude panning”, *Journal of the Audio Engineering Society*, **45**(6), pp. 456-466, June 1997.
- [9] Berkhout A. J. , de Vries D. and Vogel P., “Acoustic Control By Wave Field Synthesis”, *Journal of Acoustical Society of America*, vol. 93, pp 2764-2778, 1993
- [10] Gröhn M., Lokki T., and Takala T., “Localizing sound sources in a cave-like virtual environment with loudspeaker array reproduction”, *Presence: Teleoperators & Virtual Environments*, **16**(2), pp. 157-171, April 2007.
- [11] Begault D., “3D sound for virtual reality and multimedia”, Cambridge, MA: Academic Press, 1994.
- [12] Corteel E., “Equalization in an extended area using multichannel inversion and wave field synthesis”, *Journal of the Audio Engineering Society*, **54**(12), pp. 1140-1161, December 2006
- [13] Fröhlich B., Blach R., Stefani O., “Implementing Multi-Viewer Stereo Displays”, *WSCG Conference Proceedings*, Plzen, Czech Republic, 2005.
- [14] Boone M. M., “Multi-actuator Panels as loudspeakers arrays for Wave Field Synthesis”, *Journal of the Audio Engineering Society*, **52**(7/8), pp. 712-723, July-August 2004.

- [15] Cordeel E., “Objective and subjective comparison of electrodynamic and MAP loudspeakers for Wave Field Synthesis” *30th International Conference of the Audio Engineering Society*, Saariselkä, Finland, 2007.
- [16] Pueo B., Escolano J., Javier Lopez J., Ramos G., “On Large Multiactuator Panels for Wave Field Synthesis Applications”, *124th Convention of the Audio Engineering Society*, Amsterdam, The Netherlands, 2008.
- [17] Cordeel E. ”On the use of irregularly spaced loudspeaker arrays for Wave Field Synthesis, potential impact on spatial aliasing frequency” *9th Int. Conference on Digital Audio Effects (DAFx-06)*, Montreal, Canada, 2006.
- [18] Cordeel E., Pellegrini R., Kuhn-Rahloff C., “Wave Field Synthesis with Increased Aliasing Frequency”, *124th Convention of the Audio Engineering Society*, Amsterdam, Netherland, 2008.
- [19] Sanson J., Cordeel E., Warusfel O., “Objective and subjective analysis of localization accuracy in Wave Field Synthesis”, *124th Convention of the Audio Engineering Society*, Amsterdam, Netherland, 2008.
- [20] Stern R. M. , Zeitberg A. S., and Trahiotis C., “Lateralization of complex binaural stimuli, a weighted-image model”, *Journal of the Acoustical Society of America*, 84(1), pp. 156-165, 1988.
- [21] Jacquemin C., “Architecture and Experiments in networked 3D Audio/Graphic rendering with Virtual Choreographer”, *Proceedings of Sounds and Music Computing*, Paris, France, 2004.
- [22] Jacquemin C., “Virtual Choreographer Reference Guide (version 1.4)”, LIMSI-CNRS and Université Paris 11 <http://virchor.sourceforge.net>
- [23] Zicarelli D., Taylor G., Clayton J.K., Dudas R., Nevil B., “MAX 4.6: Reference Manual”, <http://www.cycling74.com>
- [24] Bouchara T., “Le Scene-Modeler: Des outils pour la modélisation de contenus multimedia spatialisés.” *Actes des 13 èmes Journées d’Informatique Musicale*, Albi, France, 2008. <http://gmea.net/upload/>
- [25] Burbeck S., “Applications Programming in Smalltalk-80(TM): How to use Model-View-Controller (MVC)” *Ph.D. thesis*, University of Illinois at Urbana-Champaign, 1987.
- [26] Blauert J., “Spatial Hearing, the Psychophysics of Human Sound Localization”, MIT Press, first published in 1974, re-edited in 1997.
- [27] Bertelson P., Aschersleben G., “Automatic visual bias of perceived auditory location”, *Psychonomic Bulletin & Review*, 5(3), pp. 482-489, 1998.
- [28] Wightman F. L., Kistler, D. J. “The dominant role of low-frequency interaural time differences in sound localization” *Journal of the Acoustical Society of America*, 91(3), pp. 1648-1641, 1992.
- [29] Verheijen E., “Sound reproduction by Wave Field Synthesis”, *Ph.D. thesis*, Delft University of Technology, 1997.
- [30] Bertet S., Daniel J., Parizet E., Gros L., Warusfel O., “Investigation of the perceived spatial resolution of higher ambisonics sound fields: a subjective evaluation involving virtual and real 3D microphones”, *30th International Conference of the Audio Engineering Society*, Saariselkä, Finland, 2007.
- [31] Nguyen K. V., Suied C., Viaud-Delmon I., Warusfel O., “Intergrating visual and auditory spatial cues in a virtual reality environment”, *Submitted*.
- [32] Wightman F. L., Kistler D. J., “Headphone simulation of free-field listening II: Psychophysical validation.”, *The Journal of Acoustical Society of America*, 85(2), pp. 868-878, 1989.

- [33] Bronkhorst A., “Localization of real and virtual sound sources”, *The Journal of the Acoustical Society of America*, **98**(1), pp. 2542-2553, 1995.
- [34] Speigle, J. M., Loomis, J. M., “Auditory distance perception by translating observers”, *Proceedings of IEEE Symposium on Research Frontiers in Virtual Reality*, San Jose, CA, October 25-26, 1993.
- [35] Ashmead D.H., Deford L.D., Northington A. “Contribution of listener’s approaching motion to auditory distance perception”, *Journal of Experimental Psychology: Human Perception and Performance*, **21**(2),pp. 239-256, 1995.
- [36] Creem-Regehr S. H., Willemsen P., Gooch A. A., Thompson W. B. “The influence of restricted viewing conditions on egocentric distance perception: Implications for real and virtual indoor environments”, *Perception* **34**(2), pp. 191-204, 2005.